

Size-dependent free vibration and dynamic analyses of a sandwich microbeam based on higher-order sinusoidal shear deformation theory and strain gradient theory

Mohammad Arefi^{*1}, Elyas Mohammad-Rezaei Bidgoli¹ and Ashraf M. Zenkour^{2,3}

¹Department of Solid Mechanics, Faculty of Mechanical Engineering, University of Kashan, Kashan 87317-51167, Iran

²Department of Mathematics, Faculty of Science, King Abdulaziz University, Jeddah 21589, Saudi Arabia

³Department of Mathematics, Faculty of Science, Kafrelsheikh University, Kafrelsheikh 33516, Egypt

(Received April 25, 2017, Revised May 18, 2018, Accepted May 28, 2018)

Abstract. The governing equations of motion are derived for analysis of a sandwich microbeam in this paper. The sandwich microbeam is including an elastic micro-core and two piezoelectric micro-face-sheets. The microbeam is subjected to transverse loads and two-dimensional electric potential. Higher-order sinusoidal shear deformation beam theory is used for description of displacement field. To account size dependency in governing equations of motion, strain gradient theory is used to mention higher-order stress and strains. An analytical approach for simply-supported sandwich microbeam with short-circuited electric potential is proposed. The numerical results indicate that various types of parameters such as foundation and material length scales have significant effects on the free vibration responses and dynamic results. Investigation on the influence of material length scales indicates that increase of both dimensionless material length scale parameters leads to significant changes of vibration and dynamic responses of microbeam.

Keywords: sandwich microbeam; piezoelectric face-sheets; micro-length-scale parameters; strain gradient theory; Pasternak's foundation

1. Introduction

The scientists have found this fact that the behavior of materials in very small scales leads to important changes in fundamental governing equations and need more considerations. These changes for different analyses such as free vibration, wave propagation, extension and other analyses presents different behaviors. To capture the effect of various parameters in micro- and nano-scale, some new theories have been developed. Eringen (1983) developed nonlocal elasticity for nano-scale problems and Wang *et al.* (2010) developed strain gradient theory for micro-scale problems. Studying the behavior of a micro-sandwich beam can present important issues for researchers. A literature review on micro-scale problems can be presented as follows.

Wang (2010) used Timoshenko's beam theory to study the effect of transverse shear deformation on the deflection and stress resultants of single-span Timoshenko's beams, with general loading and boundary conditions. A modified couple stress theory has been developed by Park and Gao (2006) to study bending analysis of a Bernoulli–Euler beam using principle of minimum total potential energy. They investigated the influence of material length scale parameters on the results. It was concluded that employing the new model for micro-scale problems leads to a more rigid structure rather than classical models. Aydogdu (2009)

presented axial vibration analysis of nanorods with clamped-clamped and clamped–free boundary conditions. He investigated that considering the nonlocal parameter leads to increase in natural frequencies of nanorods.

The wave propagating in 1D nano-structures with initial axial stress has been investigated by Song *et al.* (2010). They used a nonlocal elastic model incorporating with strain gradient theory. Buckling nonlocal analysis of a micro- or nano-rods/tubes was studied by Ghannadpour and Mohammadi (2010) using the Eringen's nonlocal elasticity theory based on the Timoshenko beam theory. Shooshtari and Rafiee (2011) studied nonlinear forced vibration analysis of a FG beam using Euler–Bernoulli beam theory. The nonlinearity was assumed based on von Kármán relations. Both exponentially and power law distributions have been used for gradation of material properties along the thickness direction. Firstly, Galerkin method was used to obtain a second-order nonlinear ordinary equation with cubic nonlinear term and finally multiple time scale solutions were developed. Pradhan and Chakraverty (2013) presented free vibration analysis of functionally graded beams subjected to various types of boundary conditions based on classical and first order shear deformation beam theories. The influence of some important parameters such as constituent volume fractions, slenderness ratios and the beam theories has been studied on the vibration characteristics of the problem. Sahmani and Ansari (2013) studied vibration responses of functionally graded microplates. Mori–Tanaka homogenization technique was used for description of gradation of material properties. The

*Corresponding author, Assistant Professor
E-mail: arefi63@gmail.com

governing equations of motion and constitutive relations have been derived using strain gradient elasticity theory with three material length scale parameters for accounting the size dependencies. They were concluded that by approaching the thickness of microplates to the value of internal material length scale parameter, the natural frequency increases significantly. The one dimensional wave propagation in a nanobar has been presented by Güven (2014). The local and nonlocal solutions were evaluated for wave velocity.

Size-dependent analysis of nano-structures was studied by many researchers (Belkorissat *et al.* 2015, Larbi Chaht *et al.* 2015, Ahouel *et al.* 2016, Bouafia *et al.* 2017). They examined the influence of various shear deformation theory on the nonlocal analysis of nanobeams and plates. Sandwich structures can be used in various situations to perform a defined operation and withstand against various loads. Analysis of sandwich structures needs more consideration rather than single layered structures. Application of higher-order shear deformation theory for sandwich structures was performed by various researchers (Tounsi *et al.* 2013, Boudierba *et al.* 2016). The effect of temperature rising and temperature dependencies was studied on the vibration and bending results of functionally graded structures based on various higher-order shear deformation theory (Attia *et al.* 2015, Bourada *et al.* 2015, Houari *et al.* 2016, Bousahla *et al.* 2016, Beldjelili *et al.* 2016). Some applications of sandwich structure and analysis of them were investigated by Mahi *et al.* (2015), Ait Amar Meziane *et al.* (2014), Menasria *et al.* (2017), Bennoun *et al.* (2016), Hamidi *et al.* (2015), Abdelaziz *et al.* (2017), El-Haina *et al.* (2017), Abualnour *et al.* (2018). In addition, the comprehensive analysis of nano and micro structures was reported by Zemri *et al.* (2015), Bounouara *et al.* (2016), Besseghier *et al.* (2017), Al-Basyouni *et al.* (2015), Khetir *et al.* (2017), Mouffoki *et al.* (2017), Bellifa *et al.* (2017), Larbi Chaht *et al.* (2015). Arefi *et al.* (2011) studied the influence of magnetic field on the responses of a smart cylindrical shell. Some application of piezoelectric materials as sensor and actuator can be observed in literature (Arefi and Rahimi 2011a,b, 2012a,b,c, 2014a,b, Arefi *et al.* 2012, Arefi 2014, 2015, Arefi and Allam 2015, Rahimi *et al.* 2012, Arefi *et al.* 2016a,b,c, Arefi 2018a,b, Khoshgoftar *et al.* 2013).

Farokhi and Ghayesh (2015) developed the nonlinear equations of motion for micro-arches under axial loads using the modified couple stress theory. Sourki and Hoseini (2016) developed modified couple stress theory to a Euler–Bernoulli beam for vibration analysis of a cracked microbeam. The cracked beam was modeled by dividing the beam into two segments connected by a rotational spring located at the cracked section. Some useful works on the influence of magnetic and electric loads on the transient and bending responses of small scale structures were performed by Arefi and Zenkour (2016a,b,c, 2017a,b,c,d,e,f,j) and Arefi *et al.* (2017). Zhen (2016) studied vibration and instability analysis of a double-carbon nanotube system including fluid-conveying using nonlocal elasticity theory and Euler–Bernoulli beam theory. The influence of nonlocal parameter was discussed on the in-phase and out-of-phase

vibration characteristics of structure. Farajpour *et al.* (2016) studied local and nonlocal analysis of large amplitude vibration of a piezo-magnetic nanoplate subjected to applied electric and magnetic potentials. The influence of initial electric and magnetic potentials was studied on the responses of nanoplate. Arefi and Zenkour (2017c) studied two-variable sinusoidal shear deformation theory to investigate nonlocal electro-elastic analysis of a sandwich nanoplate including Kelvin-Voigt core and face-sheets. Arefi and Zenkour (2017e) studied piezo-magnetic analysis of a Timoshenko nanobeam using nonlocal magneto-electro-elastic relations. Zhang *et al.* (2017) studied size dependencies, surface and bulk effects in modeling a nanobeam based on Bernoulli-Euler and Timoshenko beam theories. They investigated that employing current model leads to significant differences in various responses such as deflection, rotation, and natural frequency. Arefi (2016a,b) studied wave propagation analysis of nanorods made from piezoelectric and magneto-electro-elastic materials respectively. Zenkour and Arefi (2017) studied the influence of applied voltage and nonlocal parameter on the free vibration and wave propagation of nanoplate and nanorods respectively.

Based on above literature review, one can conclude that there is no comprehensive work on the electro-elastic dynamic analysis of sandwich nanobeam subjected to applied electric potential using higher-order shear deformation theory. In this paper, we develop electro-elastic relations for a sandwich piezoelectric microbeam resting on Pasternak's foundation subjected to transverse loads and applied voltage. Higher-order sinusoidal shear deformation theory and strain gradient theory are used to derive the governing equations of motion. The problem is solved using analytical approach for a simply-supported microbeam. The influence of important parameters such as material length scale parameters, two parameters of Pasternak's foundation and applied voltage is studied on the vibration and dynamic characteristics. This paper is a comprehensive extension of previous work (Arefi and Zenkour 2017a) on magneto-electro-elastic analysis of sandwich nanobeam to sandwich microbeam using strain gradient theory and higher-order sinusoidal shear deformation theory. The previous paper (Arefi and Zenkour 2017a) employed first order shear deformation theory for free vibration and bending analysis of microbeam. In this work we develop the governing equations based on an advanced theory to enrich previous numerical results and conclusion. The numerical results in this paper and comparison with previous papers indicate that this work has sufficient novelty for presentation as a new work. The considered model can be used as sensor or actuator in micro- or nano-electro mechanical systems. Designer can use this model to measure loads or deflections and control the stresses or deformations using a feedback system based on two piezoelectric layers.

2. Basic relations

In this paper, we consider a sandwich microbeam with length L including a core and two piezoelectric face-sheets

with thickness h, h_p , respectively. The piezoelectric face-sheets are subjected to applied voltage V_0 . Based on the sinusoidal shear deformation theory, the displacement field components are derived as (Arefi and Zenkour 2016b)

$$\begin{aligned} u_1(x_1, x_3, t) &= u(x_1, t) - x_3 \vartheta(x_1, t) + \chi(x_3) \Gamma(x_1, t), \\ u_3(x_1, x_3, t) &= w(x_1, t) \end{aligned} \quad (1)$$

in which (u_1, u_3) are displacement components along the longitudinal and transverse directions, respectively (Fig. 1). In addition, Γ corresponding terms of higher-order shear deformation theory and $\chi(x_3)$ is a function that describes the displacement field along the thickness direction. In this study, based on the sinusoidal shear deformation theory, $\chi(x_3)$ is selected as (Fig. 1)

$$\chi(x_3) = \frac{h}{\pi} \sin\left(\frac{\pi x_3}{h}\right) \quad (2)$$

Referring to assumed displacement field in Eq. (1), the nonzero strain components are derived as

$$\begin{aligned} \varepsilon_{11} &= \frac{du}{dx_1} - x_3 \frac{d\vartheta}{dx_1} + \chi \frac{d\Gamma}{dx_1}, \\ \varepsilon_{13} &= \frac{1}{2} \left(\frac{dw}{dx_1} - \vartheta + \frac{d\chi}{dx_3} \Gamma \right) \end{aligned} \quad (3)$$

Hooke's law using Young's E and shear G moduli yields stress-strain relations for micro-core as

$$\begin{aligned} \sigma_{11} &= E \left(\frac{du}{dx_1} - x_3 \frac{d\vartheta}{dx_1} + \chi \frac{d\Gamma}{dx_1} \right), \\ \sigma_{13} &= G \left(\frac{dw}{dx_1} - \vartheta + \frac{d\chi}{dx_3} \Gamma \right) \end{aligned} \quad (4)$$

The constitutive relations for piezoelectric micro-face-sheets are derived as

$$\begin{aligned} \sigma_{11} &= C_{1111} \varepsilon_{11} - e_{113} E_3, \\ \sigma_{13} &= C_{1313} \varepsilon_{13} - e_{131} E_1 \end{aligned} \quad (5)$$

in which C_{ijkl} are stiffness coefficients, e_{ijk} are piezoelectric constants and E_k is electric field. By considering the electric potential, the constitutive relations can be completed. A two-dimensional electric potential with an applied voltage is employed as following format (Arefi and Zenkour 2017a, b)

$$\tilde{\psi}(x_1, x_3) = 2V_0 \frac{\tilde{x}_3}{h_p} - \psi(x_1) \cos\left(\frac{\pi \tilde{x}_3}{h_p}\right) \quad (6)$$

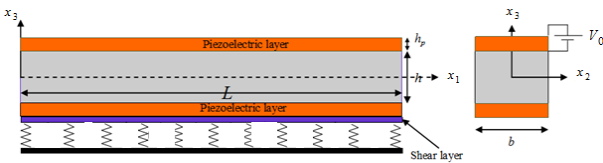


Fig. 1 The schematic of a sandwich microbeam subjected to applied voltage

where V_0 is applied voltage at top of the plate and $\tilde{x}_3 = x_3 \pm \frac{h}{2} \pm \frac{h_p}{2}$. For above electric potential, two electric potential fields are derived as

$$\begin{aligned} E_1 &= -\frac{\partial \tilde{\psi}}{\partial x_1} = \frac{d\psi}{dx_1} \cos\left(\frac{\pi \tilde{x}_3}{h_p}\right), \\ E_3 &= -\frac{\partial \tilde{\psi}}{\partial x_3} = -\frac{2V_0}{h_p} - \frac{\pi}{h_p} \psi \sin\left(\frac{\pi \tilde{x}_3}{h_p}\right) \end{aligned} \quad (7)$$

Substitution of electric potential components into stress relations yields following relations

$$\begin{aligned} \sigma_{11} &= C_{1111} \left(\frac{du}{dx_1} - x_3 \frac{d\vartheta}{dx_1} + \chi \frac{d\Gamma}{dx_1} \right) + e_{113} \left[\frac{2V_0}{h_p} + \frac{\pi}{h_p} \psi \sin\left(\frac{\pi \tilde{x}_3}{h_p}\right) \right], \\ \sigma_{13} &= C_{1313} \left(\frac{dw}{dx_1} - \vartheta + \frac{d\chi}{dx_3} \Gamma \right) - e_{131} \frac{d\psi}{dx_1} \cos\left(\frac{\pi \tilde{x}_3}{h_p}\right) \end{aligned} \quad (8)$$

For an electromechanical system, electric displacements $D_i = e_{ijk} \varepsilon_{jk} + \eta_{ik} E_k$ can be defined as

$$\begin{aligned} D_1 &= e_{113} \left(\frac{dw}{dx_1} - \vartheta \right) + \eta_{11} \frac{d\psi}{dx_1} \cos\left(\frac{\pi \tilde{x}_3}{h_p}\right), \\ D_3 &= e_{311} \left(\frac{du}{dx_1} - x_3 \frac{d\vartheta}{dx_1} \right) - \eta_{33} \left[\frac{2V_0}{h_p} + \frac{\pi}{h_p} \psi \sin\left(\frac{\pi \tilde{x}_3}{h_p}\right) \right] \end{aligned} \quad (9)$$

In this stage, the basic relations for strain gradient theory are expressed. The mentioned relations for this purpose are defined as (Wang *et al.* 2010)

$$p_i = 2\mu l_0^2 \gamma_i, \tau_{ijk} = 2\mu l_1^2 \eta_{ijk}, m_{ij} = 2\mu l_2^2 \chi_{ij} \quad (10)$$

in which p_i are stress couples, τ_{ijk} and m_{ij} are higher-order stress tensors, η_{ijk} and χ_{ij} are deviatoric stretch gradient tensor and symmetric gradient rotation tensor and γ_i is dilatation gradient tensor. In addition, μ is the bulk shear modulus and l_0, l_1 and l_2 are micro-length-scale parameters. In Eq. (10), the deviatoric stretch gradient tensor, symmetric gradient rotation tensor and corresponding dilatation are defined as (Wang *et al.* 2010)

$$\begin{aligned} \gamma_i &= \frac{\partial \varepsilon_{kk}}{\partial x_i}, \\ \eta_{ijk} &= \eta_{ijk}^s - \frac{1}{5} (\delta_{ij} \eta_{mmk}^s + \delta_{jk} \eta_{mmi}^s + \delta_{ki} \eta_{mmj}^s), \\ \chi_{ij} &= \frac{1}{4} \left(\epsilon_{ipq} \frac{\partial \varepsilon_{qj}}{\partial x_p} + \epsilon_{jpr} \frac{\partial \varepsilon_{ri}}{\partial x_p} \right) \end{aligned} \quad (11)$$

in which $\eta_{ijk}^s = \frac{1}{3} \left(\frac{\partial^2 u_i}{\partial x_j \partial x_k} + \frac{\partial^2 u_j}{\partial x_k \partial x_i} + \frac{\partial^2 u_k}{\partial x_i \partial x_j} \right)$ and ϵ_{ijk} is the permutation symbol. By using the displacement field defined in Eq. (1), the nonzero higher-order strains η_{ijk}^s and consequently η_{mmk}^s can be derived as

$$\begin{aligned} \eta_{111}^s &= \frac{d^2 u}{dx_1^2} - x_3 \frac{d^2 \vartheta}{dx_1^2} + \chi \frac{d^2 \Gamma}{dx_1^2}, & \eta_{133}^s &= \frac{1}{3} \chi'' \Gamma, \\ \eta_{113}^s &= \eta_{311}^s = \eta_{311}^s = \frac{1}{3} \left(-2 \frac{d\vartheta}{dx_1} + 2\chi \frac{d\Gamma}{dx_1} + \frac{d^2 w}{dx_1^2} \right), \\ \eta_{mm1}^s &= \eta_{111}^s + \eta_{221}^s + \eta_{331}^s = \frac{d^2 u}{dx_1^2} - x_3 \frac{d^2 \vartheta}{dx_1^2} + \chi \frac{d^2 \Gamma}{dx_1^2}, \\ \eta_{mm3}^s &= \eta_{113}^s + \eta_{223}^s + \eta_{333}^s = \frac{1}{3} \left(-2 \frac{d\vartheta}{dx_1} + 2\chi \frac{d\Gamma}{dx_1} + \frac{d^2 w}{dx_1^2} \right) \end{aligned} \quad (12)$$

After derivation of higher-order strains, we will get η_{ijk} , χ_{ij} (deviatoric stretch gradient tensor and symmetric gradient rotation tensor) and γ_i (dilatation gradient tensor) as

$$\gamma_1 = \frac{d^2u}{dx_1^2} - x_3 \frac{d^2\theta}{dx_1^2} + \chi \frac{d^2\Gamma}{dx_1^2}, \gamma_3 = -\frac{d\theta}{dx_1} + \chi' \frac{d\Gamma}{dx_1} \quad (13a)$$

$$\begin{aligned} \eta_{111} &= \eta_{111}^s - \frac{3}{5} \eta_{mm1}^s = \frac{2}{5} \left(\frac{d^2u}{dx_1^2} - x_3 \frac{d^2\theta}{dx_1^2} + \chi \frac{d^2\Gamma}{dx_1^2} \right), \\ \eta_{333} &= \eta_{333}^s - \frac{3}{5} \eta_{mm3}^s = -\frac{1}{5} \left(-2 \frac{d\theta}{dx_1} + 2\chi \frac{d\Gamma}{dx_1} + \frac{d^2w}{dx_1^2} \right), \\ \eta_{122} &= \eta_{212} = \eta_{221} = -\frac{1}{5} \left(\frac{d^2u}{dx_1^2} - x_3 \frac{d^2\theta}{dx_1^2} + \chi \frac{d^2\Gamma}{dx_1^2} \right), \\ \eta_{133} &= \eta_{313} = \eta_{331} = \frac{1}{3} \chi'' \Gamma - \frac{1}{5} \left(\frac{d^2u}{dx_1^2} - x_3 \frac{d^2\theta}{dx_1^2} + \chi \frac{d^2\Gamma}{dx_1^2} \right), \\ \eta_{113} &= \eta_{131} = \eta_{311} = \frac{4}{15} \left(-2 \frac{d\theta}{dx_1} + 2\chi \frac{d\Gamma}{dx_1} + \frac{d^2w}{dx_1^2} \right), \\ \eta_{322} &= \eta_{223} = \eta_{232} = -\frac{1}{15} \left(-2 \frac{d\theta}{dx_1} + 2\chi \frac{d\Gamma}{dx_1} + \frac{d^2w}{dx_1^2} \right) \end{aligned} \quad (13b)$$

$$\chi_{12} = \frac{1}{4} \left(\frac{\partial \varepsilon_{11}}{\partial x_3} - \frac{\partial \varepsilon_{31}}{\partial x_1} \right) = \frac{1}{8} \left(-\frac{d\theta}{dx_1} + \chi' \frac{d\Gamma}{dx_1} - \frac{d^2w}{dx_1^2} \right) \quad (13c)$$

After derivation of required terms for γ_i , χ_{ij} and η_{ijk} , the corresponding stress components p_i , m_{ij} and τ_{ijk} can be derived as

$$\begin{aligned} p_1 &= 2\mu l_0^2 \left(\frac{d^2u}{dx_1^2} - x_3 \frac{d^2\theta}{dx_1^2} + \chi \frac{d^2\Gamma}{dx_1^2} \right), \\ p_3 &= 2\mu l_0^2 \left(-\frac{d\theta}{dx_1} + \chi' \frac{d\Gamma}{dx_1} \right) \end{aligned} \quad (14a)$$

$$\begin{aligned} \tau_{111} &= \frac{4}{5} \mu l_1^2 \left(\frac{d^2u}{dx_1^2} - x_3 \frac{d^2\theta}{dx_1^2} + \chi \frac{d^2\Gamma}{dx_1^2} \right), \\ \tau_{333} &= -\frac{2}{5} \mu l_1^2 \left(-2 \frac{d\theta}{dx_1} + 2\chi \frac{d\Gamma}{dx_1} + \frac{d^2w}{dx_1^2} \right), \\ \tau_{122} &= \tau_{212} = \tau_{221} = -\frac{2}{5} \mu l_1^2 \left(\frac{d^2u}{dx_1^2} - x_3 \frac{d^2\theta}{dx_1^2} + \chi \frac{d^2\Gamma}{dx_1^2} \right), \\ \tau_{133} &= \tau_{313} = \tau_{331} = 2\mu l_1^2 \left[\frac{1}{3} \chi'' \Gamma - \frac{1}{5} \left(\frac{d^2u}{dx_1^2} - x_3 \frac{d^2\theta}{dx_1^2} + \chi \frac{d^2\Gamma}{dx_1^2} \right) \right], \\ \tau_{113} &= \tau_{131} = \tau_{311} = \frac{8}{15} \mu l_1^2 \left(-2 \frac{d\theta}{dx_1} + 2\chi \frac{d\Gamma}{dx_1} + \frac{d^2w}{dx_1^2} \right), \\ \tau_{223} &= \tau_{232} = \tau_{322} = -\frac{2}{15} \mu l_1^2 \left(-2 \frac{d\theta}{dx_1} + 2\chi \frac{d\Gamma}{dx_1} + \frac{d^2w}{dx_1^2} \right) \end{aligned} \quad (14b)$$

$$m_{12} = \frac{1}{4} \mu l_2^2 \left(-\frac{d\theta}{dx_1} + \chi' \frac{d\Gamma}{dx_1} - \frac{d^2w}{dx_1^2} \right) \quad (14c)$$

After derivation of the required expressions for stresses, electric displacements and higher-order stresses corresponding to strain gradient theory, equations of motion can be derived using Hamilton's principle $\delta \int (T - U + W) dt = 0$, in which

$$\delta T = \int \rho \dot{u}_i \delta \dot{u}_i dV, \quad ,$$

$$\delta U = \int (p_i \delta \gamma_i + \sigma_{ij} \delta \varepsilon_{ij} + \tau_{ijk} \delta \eta_{ijk} + m_{ij} \delta \chi_{ij} - D_i \delta E_i) dV \quad (15)$$

$$\delta W = \int b(q \delta u_3|_{x_3=h/2} - R_f \delta u_3|_{x_3=-h/2}) dx_1, u_3,$$

$$R_f = K_1 w - K_2 \nabla^2 w + K_3 \frac{dw}{dt}$$

where K is kinetic energy of structure, U is strain energy and W is the work performed by external works.

Kinetic energy of sandwich microbeam is expressed as

$$\begin{aligned} T &= \frac{1}{2} \int \rho \dot{u}_i^2 dV = \int \left\{ \frac{1}{2} J_1 \left[\left(\frac{du}{dt} \right)^2 + \left(\frac{dw}{dt} \right)^2 \right] - J_2 \left(\frac{du}{dt} \right) \left(\frac{d\theta}{dt} \right) \right. \\ &\quad + \frac{1}{2} J_3 \left(\frac{d\theta}{dt} \right)^2 + \frac{1}{2} \chi^2 \left(\frac{d\Gamma}{dt} \right)^2 \\ &\quad \left. + J_5 \left(\frac{du}{dt} \right) \left(\frac{d\Gamma}{dt} \right) - J_6 \left(\frac{d\theta}{dt} \right) \left(\frac{d\Gamma}{dt} \right) \right\} dx_1 \end{aligned} \quad (16)$$

in which the integration constants are expressed as

$$J_i = \int_{-\frac{h}{2}}^{\frac{h}{2}} \rho x_3^{i-1} dx_3, \quad (i = 1, 2, 3),$$

$$J_4 = \int_{-h/2}^{h/2} \rho \chi^2 dx_3, J_5 = \int_{-h/2}^{h/2} \rho \chi dx_3, \quad (17)$$

$$J_6 = \int_{-h/2}^{h/2} \rho x_3 \chi dx_3.$$

Variation of kinetic energy and energy due to external works are derived as

$$\begin{aligned} \delta T &= \int \left\{ J_1 \left[\left(\frac{du}{dt} \right) \left(\frac{d\delta u}{dt} \right) + \left(\frac{dw}{dt} \right) \left(\frac{d\delta w}{dt} \right) \right] - J_2 \left(\frac{du}{dt} \right) \left(\frac{d\delta \theta}{dt} \right) - \right. \\ &\quad \left. J_2 \left(\frac{d\theta}{dt} \right) \left(\frac{d\delta u}{dt} \right) + J_3 \left(\frac{d\theta}{dt} \right) \left(\frac{d\delta \theta}{dt} \right) \right. \\ &\quad \left. + J_4 \left(\frac{d\Gamma}{dt} \right) \left(\frac{d\delta \Gamma}{dt} \right) + J_5 \left(\frac{du}{dt} \right) \left(\frac{d\delta \Gamma}{dt} \right) + J_5 \left(\frac{d\Gamma}{dt} \right) \left(\frac{d\delta u}{dt} \right) - \right. \\ &\quad \left. J_6 \left(\frac{d\theta}{dt} \right) \left(\frac{d\delta \Gamma}{dt} \right) - J_6 \left(\frac{d\Gamma}{dt} \right) \left(\frac{d\delta \theta}{dt} \right) \right\} dx_1, \end{aligned} \quad (18a)$$

$$\delta W = \int (q_0 - R_f) \delta w dx_1, \quad (18b)$$

$$R_f = K_1 w - K_2 \nabla^2 w + K_3 \frac{dw}{dt}$$

By using Eq. (15) and integration along the thickness direction, the variation of strain energy after integration by parts is derived as

$$\begin{aligned} \delta T &= \int \left\{ J_1 \left[-\left(\frac{d^2u}{dt^2} \right) \delta u - \left(\frac{d^2w}{dt^2} \right) \delta w \right] + J_2 \left(\frac{d^2u}{dt^2} \right) \delta \theta + J_2 \left(\frac{d^2\theta}{dt^2} \right) \delta u \right. \\ &\quad \left. - J_3 \left(\frac{d^2\theta}{dt^2} \right) \delta \theta - J_4 \left(\frac{d^2\Gamma}{dt^2} \right) \delta \Gamma - J_5 \left(\frac{d^2u}{dt^2} \right) \delta \Gamma - J_5 \left(\frac{d^2\Gamma}{dt^2} \right) \delta u + \right. \\ &\quad \left. J_6 \left(\frac{d^2\theta}{dt^2} \right) \delta \Gamma + J_6 \left(\frac{d^2\Gamma}{dt^2} \right) \delta \theta \right\} dx_1 \end{aligned} \quad (19)$$

Substitution of variation of strains $\delta \varepsilon_{ij}$, dilatation gradient tensor $\delta \gamma_i$, deviatoric stretch gradient tensor $\delta \eta_{ijk}$, symmetric rotation gradient tensor $\delta \chi_{ij}$ and electric field δE_i into variation form of energy equation and integration by part on the derived equation yields

$$\begin{aligned}
\delta U = \int & \left\{ p_1 \left(\frac{d^2 \delta u}{dx_1^2} - x_3 \frac{d^2 \delta \vartheta}{dx_1^2} + \chi \frac{d^2 \delta \Gamma}{dx_1^2} \right) + p_3 \left(-\frac{d \delta \vartheta}{dx_1} + \chi' \frac{d \delta \Gamma}{dx_1} \right) \right. \\
& + \sigma_{11} \left(\frac{d \delta u}{dx_1} - x_3 \frac{d \delta \vartheta}{dx_1} + \chi \frac{d \delta \Gamma}{dx_1} \right) \\
& + \sigma_{13} \left(\frac{d \delta w}{dx_1} - \delta \vartheta + \chi' \delta \Gamma \right) + \frac{2}{5} \tau_{111} \left(\frac{d^2 \delta u}{dx_1^2} - x_3 \frac{d^2 \delta \vartheta}{dx_1^2} + \chi \frac{d^2 \delta \Gamma}{dx_1^2} \right) - \\
& \frac{1}{5} \tau_{333} \left(-2 \frac{d \delta \vartheta}{dx_1} + 2 \chi \frac{d \delta \Gamma}{dx_1} + \frac{d^2 \delta w}{dx_1^2} \right) \\
& - \frac{3}{5} \tau_{122} \left(\frac{d^2 \delta u}{dx_1^2} - x_3 \frac{d^2 \delta \vartheta}{dx_1^2} + \chi \frac{d^2 \delta \Gamma}{dx_1^2} \right) + 3 \tau_{133} \left[\frac{1}{3} \chi'' \delta \Gamma - \right. \\
& \left. \frac{1}{5} \left(\frac{d^2 \delta u}{dx_1^2} - x_3 \frac{d^2 \delta \vartheta}{dx_1^2} + \chi \frac{d^2 \delta \Gamma}{dx_1^2} \right) \right] \\
& + \frac{12}{15} \tau_{113} \left(-2 \frac{d \delta \vartheta}{dx_1} + 2 \chi \frac{d \delta \Gamma}{dx_1} + \frac{d^2 \delta w}{dx_1^2} \right) - \frac{1}{5} \tau_{223} \left(-2 \frac{d \delta \vartheta}{dx_1} + 2 \chi \frac{d \delta \Gamma}{dx_1} + \right. \\
& \left. \frac{d^2 \delta w}{dx_1^2} \right) \\
& + 2 \frac{1}{8} m_{12} \left(-\frac{d \delta \vartheta}{dx_1} + \chi' \frac{d \delta \Gamma}{dx_1} - \frac{d^2 \delta w}{dx_1^2} \right) - D_1 \cos \left(\frac{\pi \bar{x}_3}{h_p} \right) \frac{d \delta \psi}{dx_1} + \\
& \left. D_3 \frac{\pi}{h_p} \sin \left(\frac{\pi \bar{x}_3}{h_p} \right) \delta \psi \right\} dV
\end{aligned} \quad (20)$$

By substitution of $\delta \varepsilon_{ij}$, $\delta \gamma_i$, $\delta \chi_{ij}$, $\delta \eta_{ijk}$ and δE_i into Eq. (15), the variation of strain energy is derived as

$$\begin{aligned}
\delta U = \int & \left\{ \left(\frac{d^2 P_1}{dx_1^2} + \frac{2}{5} \frac{d^2 N_{111}}{dx_1^2} - \frac{3}{5} \frac{d^2 N_{133}}{dx_1^2} - \frac{d N_{11}}{dx_1} - \frac{3}{5} \frac{d^2 N_{122}}{dx_1^2} \right) \delta u - \right. \\
& \left(\frac{d^2 M_1}{dx_1^2} + \frac{2}{5} \frac{d^2 M_{111}}{dx_1^2} - \frac{d P_3}{dx_1} \right. \\
& \left. - \frac{d M_{11}}{dx_1} + \frac{2}{5} \frac{d N_{333}}{dx_1} + N_{13} - \frac{3}{5} \frac{d^2 M_{122}}{dx_1^2} - \frac{8}{5} \frac{d N_{113}}{dx_1} + \frac{2}{5} \frac{d N_{223}}{dx_1} - \right. \\
& \left. \frac{1}{4} \frac{d N_{12}^X}{dx_1} - \frac{3}{5} \frac{d^2 M_{133}}{dx_1^2} \right) \delta \vartheta \\
& + \left(-\frac{d N_{13}}{dx_1} - \frac{1}{5} \frac{d^2 N_{333}}{dx_1^2} + \frac{4}{5} \frac{d^2 N_{113}}{dx_1^2} - \frac{1}{5} \frac{d^2 N_{223}}{dx_1^2} - \frac{1}{4} \frac{d^2 N_{12}^X}{dx_1^2} \right) \delta w \\
& + \left(\frac{d^2 S_1}{dx_1^2} - \frac{d R_3}{dx_1} - \frac{d S_{11}}{dx_1} + \frac{2}{5} \frac{d^2 S_{111}}{dx_1^2} + \frac{2}{5} \frac{d S_{333}}{dx_1} + R_{13} - \frac{3}{5} \frac{d^2 S_{122}}{dx_1^2} + \right. \\
& \left. G_{133} - \frac{3}{5} \frac{d^2 S_{133}}{dx_1^2} - \frac{8}{5} \frac{d S_{113}}{dx_1} \right. \\
& \left. + \frac{2}{5} \frac{d S_{223}}{dx_1} - \frac{1}{4} \frac{d R_{12}^X}{dx_1} \right) \delta \Gamma + \left(\frac{d \bar{D}_1}{dx_1} + \bar{D}_3 \right) \delta \psi \left\} dV
\end{aligned} \quad (21)$$

in which the resultant components are expressed as

$$\begin{aligned}
N_{11} &= \int \sigma_{11} dx_3, M_{11} = \int x_3 \sigma_{11} dx_3, P_1 = \int p_1 dx_3, \\
P_3 &= \int p_3 dx_3, \\
M_1 &= \int x_3 p_1 dx_3, S_1 = \int \chi p_1 dx_3, R_3 = \int p_3 \chi' dx_3, S_{11} = \int \chi \sigma_{11} dx_3, \\
R_{13} &= \int \sigma_{13} \chi' dx_3, N_{ijk} = \int \tau_{ijk} dx_3, M_{ijk} = \int x_3 \tau_{ijk} dx_3, S_{ijk} = \\
& \int \chi \tau_{ijk} dx_3, \\
G_{ijk} &= \int \tau_{ijk} \chi'' dx_3, N_{12}^X = \int N_{12} dx_3, \\
R_{12}^X &= \int N_{12} \chi' dx_3, M_{12}^X = \int x_3 m_{12} dx_3, \\
\bar{D}_1 &= \int D_1 \cos \left(\frac{\pi \bar{x}_3}{h_p} \right) dx_3, \bar{D}_3 = \int D_3 \frac{\pi}{h_p} \sin \left(\frac{\pi \bar{x}_3}{h_p} \right) dx_3
\end{aligned} \quad (22)$$

In this stage and after completion of required terms of strain energy, kinetic energy and energy due to external works, the final governing equations of motion can be obtained by separation of coefficients of δu , δw , $\delta \vartheta$ and $\delta \psi$ as follows

$$\begin{aligned}
\delta u: & \frac{d^2 P_1}{dx_1^2} + \frac{2}{5} \frac{d^2 N_{111}}{dx_1^2} - \frac{3}{5} \frac{d^2 N_{133}}{dx_1^2} - \frac{d N_{11}}{dx_1} - \frac{3}{5} \frac{d^2 N_{122}}{dx_1^2} \\
& = -J_1 \left(\frac{d^2 u}{dt^2} \right) + J_2 \left(\frac{d^2 \vartheta}{dt^2} \right) - J_5 \left(\frac{d^2 \Gamma}{dt^2} \right)
\end{aligned} \quad (23a)$$

$$\begin{aligned}
\delta \vartheta: & -\frac{d^2 M_1}{dx_1^2} - \frac{2}{5} \frac{d^2 M_{111}}{dx_1^2} + \frac{d P_3}{dx_1} + \frac{d M_{11}}{dx_1} - \frac{2}{5} \frac{d N_{333}}{dx_1} - N_{13} + \\
& \frac{3}{5} \frac{d^2 M_{122}}{dx_1^2} + \frac{8}{5} \frac{d N_{113}}{dx_1} - \frac{2}{5} \frac{d N_{223}}{dx_1} + \frac{1}{4} \frac{d N_{12}^X}{dx_1} + \frac{3}{5} \frac{d^2 M_{133}}{dx_1^2} = \\
& J_2 \left(\frac{d^2 u}{dt^2} \right) - J_3 \left(\frac{d^2 \vartheta}{dt^2} \right) + J_6 \left(\frac{d^2 \Gamma}{dt^2} \right)
\end{aligned} \quad (23b)$$

$$\begin{aligned}
\delta w: & -\frac{d N_{13}}{dx_1} - \frac{1}{5} \frac{d^2 N_{333}}{dx_1^2} + \frac{4}{5} \frac{d^2 N_{113}}{dx_1^2} - \frac{1}{5} \frac{d^2 N_{223}}{dx_1^2} - \frac{1}{4} \frac{d^2 N_{12}^X}{dx_1^2} \\
& = -J_1 \left(\frac{d^2 w}{dt^2} \right) + q - K_1 w + K_2 \nabla^2 w - K_3 \frac{dw}{dt}
\end{aligned} \quad (23c)$$

$$\begin{aligned}
\delta \Gamma: & \frac{d^2 S_1}{dx_1^2} - \frac{d R_3}{dx_1} - \frac{d S_{11}}{dx_1} + \frac{2}{5} \frac{d^2 S_{111}}{dx_1^2} + \frac{2}{5} \frac{d S_{333}}{dx_1} + R_{13} - \frac{3}{5} \frac{d^2 S_{122}}{dx_1^2} \\
& + G_{133} - \frac{3}{5} \frac{d^2 S_{133}}{dx_1^2} - \frac{8}{5} \frac{d S_{113}}{dx_1} + \frac{2}{5} \frac{d S_{223}}{dx_1} \\
& - \frac{1}{4} \frac{d R_{12}^X}{dx_1} \\
& = -J_4 \left(\frac{d^2 \Gamma}{dt^2} \right) - J_5 \left(\frac{d^2 u}{dt^2} \right) + J_6 \left(\frac{d^2 \vartheta}{dt^2} \right)
\end{aligned} \quad (23d)$$

$$\delta \psi: \frac{d \bar{D}_1}{dx_1} + \bar{D}_3 = 0 \quad (23e)$$

By substitution of strain and electric field components into basic relations, the resultant components are derived as

$$\begin{aligned}
N_{11} &= J_7 \frac{du}{dx_1} - J_8 \frac{d\vartheta}{dx_1} + J_9 \psi + J_{23} \frac{d\Gamma}{dx_1} + N^\psi, \\
N_{13} &= J_{12} \left(\frac{dw}{dx_1} - \vartheta \right) - J_{13} \frac{d\psi}{dx_1} + J_{24} \Gamma, \\
M_{11} &= J_8 \frac{du}{dx_1} - J_{10} \frac{d\vartheta}{dx_1} + J_{11} \psi + J_{27} \frac{d\Gamma}{dx_1} + M^\psi, \\
\bar{D}_1 &= J_{13} \left(\frac{dw}{dx_1} - \vartheta \right) + J_{25} \Gamma + J_{14} \frac{d\psi}{dx_1}, \\
\bar{D}_3 &= J_9 \frac{du}{dx_1} - J_{11} \frac{d\vartheta}{dx_1} + J_{26} \frac{d\Gamma}{dx_1} - J_{15} \psi - D^\psi, \\
P_1 &= J_{16} \frac{d^2 u}{dx_1^2} - J_{17} \frac{d^2 \vartheta}{dx_1^2} + J_{28} \frac{d^2 \Gamma}{dx_1^2}, \\
P_3 &= -J_{16} \frac{d\vartheta}{dx_1} + J_{29} \frac{d\Gamma}{dx_1}, \\
M_1 &= J_{17} \frac{d^2 u}{dx_1^2} - J_{18} \frac{d^2 \vartheta}{dx_1^2} + J_{30} \frac{d^2 \Gamma}{dx_1^2}, \\
S_1 &= +J_{28} \frac{d^2 u}{dx_1^2} - J_{30} \frac{d^2 \vartheta}{dx_1^2} + J_{35} \frac{d^2 \Gamma}{dx_1^2}, \\
R_3 &= -J_{29} \frac{d\vartheta}{dx_1} + J_{36} \frac{d\Gamma}{dx_1}, \\
S_{11} &= J_{23} \frac{du}{dx_1} - J_{27} \frac{d\vartheta}{dx_1} + J_{26} \psi + J_{37} \frac{d\Gamma}{dx_1} + S^\psi, \\
R_{13} &= J_{24} \left(\frac{dw}{dx_1} - \vartheta \right) - J_{25} \frac{d\psi}{dx_1} + J_{38} \Gamma, \\
G_{133} &= \frac{1}{3} J_{43} \Gamma - \frac{1}{5} \left(J_{40} \frac{d^2 u}{dx_1^2} - J_{41} \frac{d^2 \vartheta}{dx_1^2} + J_{42} \frac{d^2 \Gamma}{dx_1^2} \right),
\end{aligned} \quad (24)$$

$$\begin{aligned}
\{N_{111}, N_{122}\} &= \frac{1}{5}\{2, -1\} \left(J_{19} \frac{d^2 u}{dx_1^2} - J_{20} \frac{d^2 \vartheta}{dx_1^2} + J_{31} \frac{d^2 \Gamma}{dx_1^2} \right), \\
\{N_{113}, N_{223}, N_{333}\} &= \frac{1}{15}\{4, -1, -1\} \left(J_{19} \frac{d^2 w}{dx_1^2} - 2J_{19} \frac{d\vartheta}{dx_1} + 2J_{31} \frac{d\Gamma}{dx_1} \right), \\
\{M_{111}, M_{122}\} &= \frac{1}{5}\{2, -1\} \left(J_{20} \frac{d^2 u}{dx_1^2} - J_{21} \frac{d^2 \vartheta}{dx_1^2} + J_{32} \frac{d^2 \Gamma}{dx_1^2} \right), \\
\{S_{111}, S_{122}\} &= \frac{1}{5}\{2, -1\} \left(J_{31} \frac{d^2 u}{dx_1^2} - J_{32} \frac{d^2 \vartheta}{dx_1^2} + J_{39} \frac{d^2 \Gamma}{dx_1^2} \right), \\
\{S_{113}, S_{223}, S_{333}\} &= \frac{1}{15}\{4, -1, -1\} \left(J_{31} \frac{d^2 w}{dx_1^2} - 2J_{31} \frac{d\vartheta}{dx_1} + 2J_{39} \frac{d\Gamma}{dx_1} \right), \\
N_{133} &= \frac{1}{3}J_{40}\Gamma - \frac{1}{5}\left(J_{19} \frac{d^2 u}{dx_1^2} - J_{20} \frac{d^2 \vartheta}{dx_1^2} + J_{31} \frac{d^2 \Gamma}{dx_1^2}\right), \\
M_{133} &= \frac{1}{3}J_{41}\Gamma - \frac{1}{5}\left(J_{20} \frac{d^2 u}{dx_1^2} - J_{21} \frac{d^2 \vartheta}{dx_1^2} + J_{32} \frac{d^2 \Gamma}{dx_1^2}\right), \\
S_{133} &= \frac{1}{3}J_{42}\Gamma - \frac{1}{5}\left(J_{31} \frac{d^2 u}{dx_1^2} - J_{32} \frac{d^2 \vartheta}{dx_1^2} + J_{39} \frac{d^2 \Gamma}{dx_1^2}\right), \\
N_{12}^x &= \frac{1}{8}J_{22} \left(-\frac{d\vartheta}{dx_1} - \frac{d^2 w}{dx_1^2} \right) + \frac{1}{8}J_{33} \frac{d\Gamma}{dx_1}, \\
R_{12}^x &= \frac{1}{8}J_{33} \left(-\frac{d\vartheta}{dx_1} - \frac{d^2 w}{dx_1^2} \right) + \frac{1}{8}J_{34} \frac{d\Gamma}{dx_1}
\end{aligned}$$

in which the integration constants are expressed in Appendix.

Substitution of resultant components into five equations of motion leads to

$$\begin{aligned}
\delta u: & \left(J_{16} + \frac{4}{25}J_{19} + \frac{3}{25}J_{19} + \frac{3}{25}J_{19} \right) \frac{d^4 u}{dx_1^4} - J_7 \frac{d^2 u}{dx_1^2} \\
& - \left(\frac{3}{25}J_{20} + J_{17} + \frac{4}{25}J_{20} + \frac{3}{25}J_{20} \right) \frac{d^4 \vartheta}{dx_1^4} + J_8 \frac{d^2 \vartheta}{dx_1^2} + \\
& \left(\frac{3}{25}J_{31} + J_{28} + \frac{4}{25}J_{31} + \frac{3}{25}J_{31} \right) \frac{d^4 \Gamma}{dx_1^4} \\
& - \left(J_{23} + \frac{1}{5}J_{40} \right) \frac{d^2 \Gamma}{dx_1^2} - J_9 \frac{d\psi}{dx_1} = \frac{dN\psi}{dx_1} - \\
& J_1 \frac{d^2 u}{dt^2} + J_2 \frac{d^2 \vartheta}{dt^2} - J_5 \frac{d^2 \Gamma}{dt^2},
\end{aligned} \quad (25a)$$

$$\begin{aligned}
\delta \vartheta: & - \left(J_{17} + \frac{3}{25}J_{20} + \frac{4}{25}J_{20} + \frac{3}{25}J_{20} \right) \frac{d^4 u}{dx_1^4} + J_8 \frac{d^2 u}{dx_1^2} \\
& + \left(\frac{3}{25}J_{21} + \frac{3}{25}J_{21} + J_{18} + \frac{4}{25}J_{21} \right) \frac{d^4 \vartheta}{dx_1^4} \\
& - \left(\frac{4}{75}J_{19} + \frac{64}{75}J_{19} + \frac{4}{75}J_{19} + J_{16} + J_{10} + \frac{1}{32}J_{22} \right) \frac{d^2 \vartheta}{dx_1^2} \\
& + J_{12}\vartheta \\
& + \left(\frac{32}{75}J_{19} + \frac{2}{75}J_{19} + \frac{2}{75}J_{19} - \frac{1}{32}J_{22} \right) \frac{d^3 w}{dx_1^3} - J_{12} \frac{dw}{dx_1} \\
& - \left(J_{30} + \frac{4}{25}J_{32} + \frac{3}{25}J_{32} + \frac{3}{25}J_{32} \right) \frac{d^4 \Gamma}{dx_1^4} \\
& + \left(\frac{64}{75}J_{31} + J_{29} + J_{27} + \frac{4}{75}J_{31} + \frac{4}{75}J_{31} + \frac{1}{32}J_{33} + \frac{1}{5}J_{41} \right) \frac{d^2 \Gamma}{dx_1^2} \\
& - J_{24}\Gamma + (J_{13} + J_{11}) \frac{d\psi}{dx_1} \\
& = -\frac{dM\psi}{dx_1} + J_2 \frac{d^2 u}{dt^2} - J_3 \frac{d^2 \vartheta}{dt^2} + J_6 \frac{d^2 \Gamma}{dt^2}
\end{aligned} \quad (25b)$$

$$\begin{aligned}
\delta w: & \left(\frac{1}{32}J_{22} - \frac{32}{75}J_{19} - \frac{2}{75}J_{19} - \frac{2}{75}J_{19} \right) \frac{d^3 \vartheta}{dx_1^3} + J_{12} \frac{d\vartheta}{dx_1} \\
& + \left(\frac{1}{32}J_{22} + \frac{16}{75}J_{19} + \frac{1}{75}J_{19} + \frac{1}{75}J_{19} \right) \frac{d^4 w}{dx_1^4} - J_{12} \frac{d^2 w}{dx_1^2} \\
& + \left(\frac{2}{75}J_{31} + \frac{32}{75}J_{31} + \frac{2}{75}J_{31} - \frac{1}{32}J_{33} \right) \frac{d^3 \Gamma}{dx_1^3} - J_{24} \frac{d\Gamma}{dx_1} + J_{13} \frac{d^2 \psi}{dx_1^2} \\
& = -J_1 \frac{d^2 w}{dt^2} + q - K_1 w + K_2 \nabla^2 w - K_3 \frac{dw}{dt} \\
\delta \Gamma: & \left(\frac{3}{25}J_{31} + J_{28} + \frac{4}{25}J_{31} + \frac{3}{25}J_{31} \right) \frac{d^4 u}{dx_1^4} - \left(J_{23} + \frac{1}{5}J_{40} \right) \frac{d^2 u}{dx_1^2} \\
& - \left(\frac{3}{25}J_{32} + \frac{3}{25}J_{32} + J_{30} + \frac{4}{25}J_{32} \right) \frac{d^4 \vartheta}{dx_1^4} - J_{24}\vartheta \\
& + \left(J_{29} + \frac{4}{75}J_{31} + \frac{1}{5}J_{41} + \frac{1}{32}J_{33} + \frac{64}{75}J_{31} + \frac{4}{75}J_{31} + J_{27} \right) \frac{d^2 \vartheta}{dx_1^2} \\
& + \left(-\frac{2}{75}J_{31} - \frac{2}{75}J_{31} - \frac{32}{75}J_{31} + \frac{1}{32}J_{33} \right) \frac{d^3 w}{dx_1^3} + J_{24} \frac{dw}{dx_1} \\
& + \left(\frac{3}{25}J_{39} + \frac{3}{25}J_{39} + \frac{4}{25}J_{39} + J_{35} \right) \frac{d^4 \Gamma}{dx_1^4} \\
& - \left(J_{36} + J_{37} + \frac{1}{5}J_{42} + \frac{1}{5}J_{42} + \frac{64}{75}J_{39} + \frac{4}{75}J_{39} + \frac{1}{32}J_{34} \right. \\
& \quad \left. + \frac{4}{75}J_{39} \right) \frac{d^2 \Gamma}{dx_1^2} \\
& + \left(J_{38} + \frac{1}{3}J_{43} \right) \Gamma - (J_{26} + J_{25}) \frac{d\psi}{dx_1} = \frac{dS\psi}{dx_1} - J_4 \frac{d^2 \Gamma}{dt^2} - \\
& J_5 \frac{d^2 u}{dt^2} + J_6 \frac{d^2 \vartheta}{dt^2}
\end{aligned} \quad (25d)$$

$$\begin{aligned}
\delta \psi: & J_9 \frac{du}{dx_1} - (J_{13} + J_{11}) \frac{d\vartheta}{dx_1} + J_{13} \frac{d^2 w}{dx_1^2} + (J_{25} + J_{26}) \frac{d\Gamma}{dx_1} \\
& + J_{14} \frac{d^2 \psi}{dx_1^2} - J_{15}\psi = D\psi
\end{aligned} \quad (25e)$$

3. Solution procedure

For free vibration and dynamic analysis of sandwich microbeam with two axially movable ends fixed along the transverse direction and two short-circuited electric potential, the following solution may be supposed as

$$\begin{cases} (u, \vartheta, \Gamma) \\ (w, \psi) \end{cases} = \sum_{n=1}^{\infty} \left\{ \begin{matrix} (U_n, \Theta_n, E_n) \cos(\lambda_n x_1) \\ (W_n, \Psi_n) \sin(\lambda_n x_1) \end{matrix} \right\} e^{i\omega t} \quad (26)$$

where $\lambda_n = n\pi/L$. Based on above solution and substitution into governing equations of motion, elements of stiffness, mass and force matrix can be obtained as

$$\{k\}\{X\} = [M]\{\ddot{X}\} + [C]\{\dot{X}\} + \{F\} \quad (27)$$

in which $\{X\} = \{U_n, \Theta_n, W_n, E_n, \Psi_n\}^T$ and the nonzero symmetric elements of stiffness k_{ij} and mass in this case can be obtained as

$$\begin{aligned}
k_{11} &= \left(J_{16} + \frac{2}{5}J_{19} \right) \lambda_n^4 + J_7 \lambda_n^2, \quad k_{12} = - \left(J_{17} + \right. \\
& \left. \frac{2}{5}J_{20} \right) \lambda_n^4 - J_8 \lambda_n^2, \quad k_{13} = 0, \quad k_{14} = \left(J_{28} + \frac{2}{5}J_{31} \right) \lambda_n^4 + \left(J_{23} + \frac{1}{5}J_{40} \right) \lambda_n^2,
\end{aligned} \quad (28)$$

$$\begin{aligned}
 k_{15} &= -J_9 \lambda_n, M_{11} = -J_1, M_{12} = J_2, M_{14} = -J_5, \\
 k_{22} &= \left(J_{18} + \frac{2}{5} J_{21} \right) \lambda_n^4 + \left(J_{10} + J_{16} + \frac{72}{75} J_{19} + \frac{1}{32} J_{22} \right) \lambda_n^2 \\
 &\quad + J_{12}, k_{23} \\
 &= - \left(\frac{36}{75} J_{19} - \frac{1}{32} J_{22} \right) \lambda_n^3 - J_{12} \lambda_n, \\
 k_{24} &= - \left(J_{30} + \frac{2}{5} J_{32} \right) \lambda_n^4 - \left(J_{27} + J_{29} + \frac{72}{75} J_{31} + \frac{1}{32} J_{33} + \right. \\
 &\quad \left. \frac{1}{5} J_{41} \right) \lambda_n^2 - J_{24} \lambda_n \\
 k_{25} &= (J_{13} + J_{11}) \lambda_n, M_{22} = -J_3, M_{24} = J_6, \\
 k_{33} &= \left(\frac{1}{32} J_{22} + \frac{18}{75} J_{19} \right) \lambda_n^4 + J_{12} \lambda_n^2 + K_1 + K_2 \lambda_n^2 \\
 k_{34} &= \left(\frac{36}{75} J_{31} - \frac{1}{32} J_{33} \right) \lambda_n^3 + J_{24} \lambda_n, k_{35} = -J_{13} \lambda_n^2, M_{33} = -J_1, \\
 k_{44} &= \left(J_{35} + \frac{2}{5} J_{39} \right) \lambda_n^4 - \left(\frac{1}{32} J_{34} + J_{36} + J_{37} + \right. \\
 &\quad \left. \frac{2}{5} J_{42} + \frac{72}{75} J_{39} \right) \lambda_n^2 + \left(J_{38} + \frac{1}{3} J_{43} \right), k_{45} = -(J_{26} + J_{25}) \lambda_n, \\
 k_{55} &= -J_{14} \lambda_n^2 - J_{15}, M_{41} = -J_5, M_{42} = J_6, M_{44} = -J_4
 \end{aligned}$$

4. Results and discussion

The numerical results of the problem including the natural frequencies and dynamic responses may be presented as function of input parameters of the problem. Before presentation of the numerical results, the material properties of core and piezoelectric face-sheets may be presented as (Arefi and Zenkour 2017a, b)

$$\begin{aligned}
 E &= 1 \times 10^{12} \text{ (Pa)}, \nu = 0.3, \rho = 2300 \text{ (kg/m}^3\text{)}, \\
 c_{1111} &= 226 \times 10^9 \text{ Pa}, c_{1212} = c_{1313} = 44.2 \times 10^9 \text{ Pa}, \\
 e_{113} &= e_{131} = -2.2 \text{ (C/m}^2\text{)}, \rho^p = 5500 \text{ (kg/m}^3\text{)}, \\
 \eta_{11} &= 5.64 \times 10^{-9} \text{ (C/mV)}, \eta_{33} = 6.35 \times 10^{-9} \text{ (C/mV)}
 \end{aligned}$$

To investigate the effect of three micro-length-scale parameters (l_0, l_1, l_2) on the dynamic results of the sandwich microbeam, two-dimensionless parameters $\alpha = l_1/l_0$ and $\beta = l_2/l_0$ are employed.

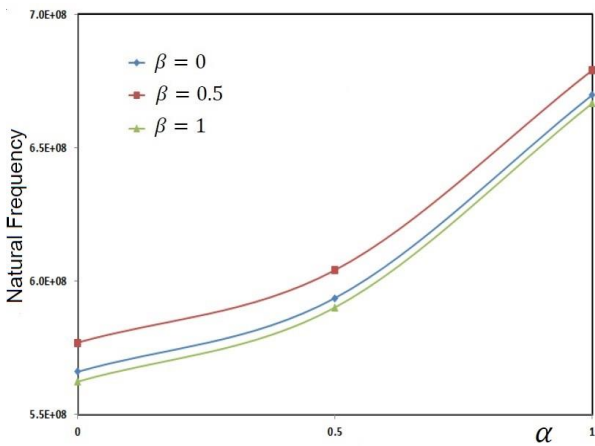


Fig. 2 Fundamental natural frequencies of sandwich microbeam in terms of two dimensionless parameters α, β

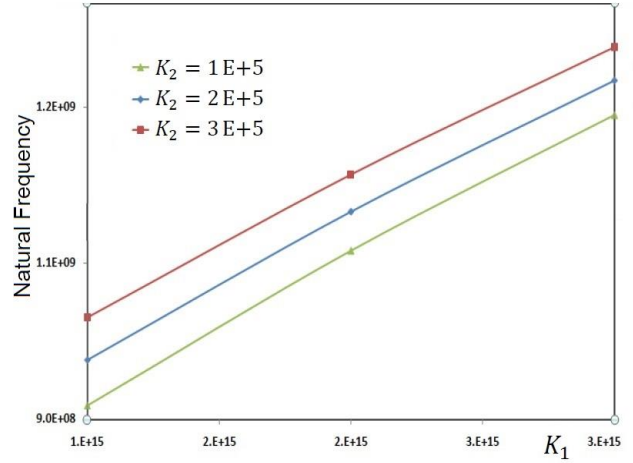


Fig. 3 Fundamental natural frequencies of sandwich microbeam in terms of two parameters of foundations K_1, K_2

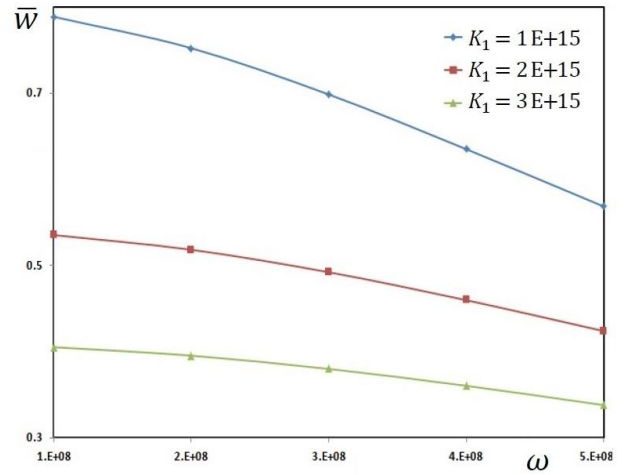


Fig. 4 The non-dimensional displacement \bar{w} of sandwich microbeam in terms of excitation frequency ω for various Winkler's parameters of foundations K_1

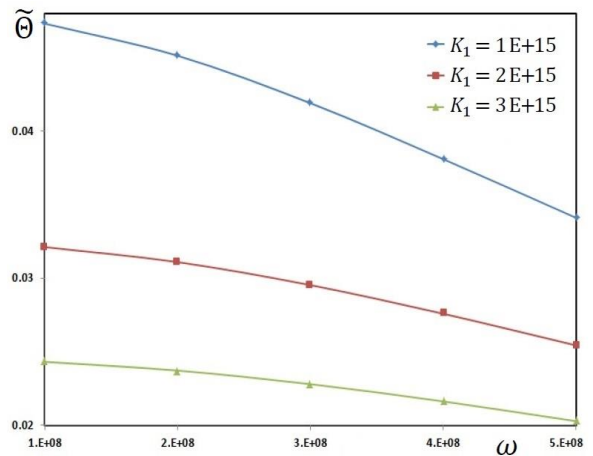


Fig. 5 The beam rotation $\tilde{\theta}$ of sandwich microbeam in terms of excitation frequency ω for various Winkler's parameters of foundations K_1

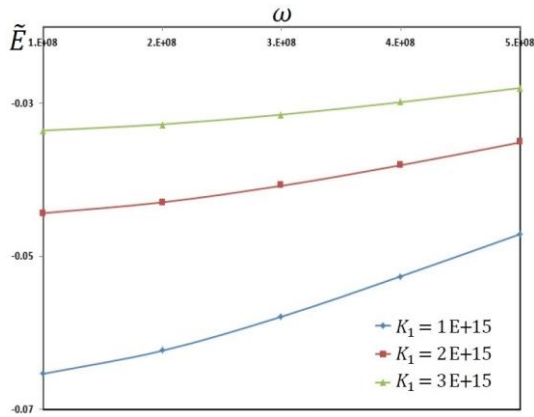


Fig. 6 The beam higher-order rotation \tilde{E} of sandwich microbeam in terms of excitation frequency ω for various Winkler's parameters of foundation K_1 .

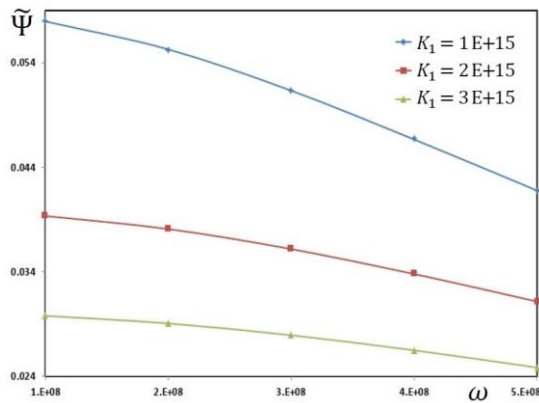


Fig. 7 The maximum electric potential $\tilde{\Psi}$ through thickness direction of sandwich microbeam in terms of excitation frequency ω for various Winkler's parameters of foundation K_1 .

Fig. 2 shows fundamental natural frequencies of sandwich microbeam in terms of two dimensionless parameters α, β . It can be observed that with increase of α , all fundamental natural frequencies are decreased significantly. In addition, the values of natural frequencies are strongly depending on the values of β . The unique and general expression for change of natural frequencies in terms of β cannot be mentioned. Figure 3 shows variation of fundamental natural frequencies of sandwich microbeam in terms of spring K_1 and shear K_2 parameters of foundation. One can conclude that fundamental natural frequencies are increased significantly with increase of both parameters. This is due increase of stiffness of foundation that leads to larger natural frequencies.

The influence of Winkler's parameters of foundation K_1 on the dynamic responses of microbeam is presented here. Shown in Fig. 4 is non-dimensional displacement $\bar{w} = 10^3 W/L$ of sandwich microbeam in terms of excitation frequency ω for various Winkler's parameters of foundation K_1 .

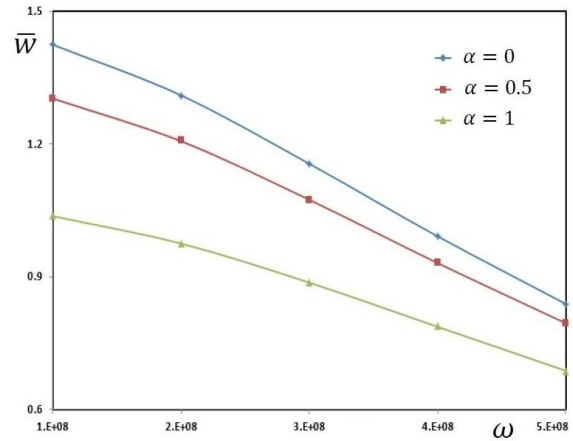


Fig. 8 The non-dimensional displacement \bar{w} of sandwich microbeam in terms of excitation frequency ω for various first dimensionless material length scale parameters α .

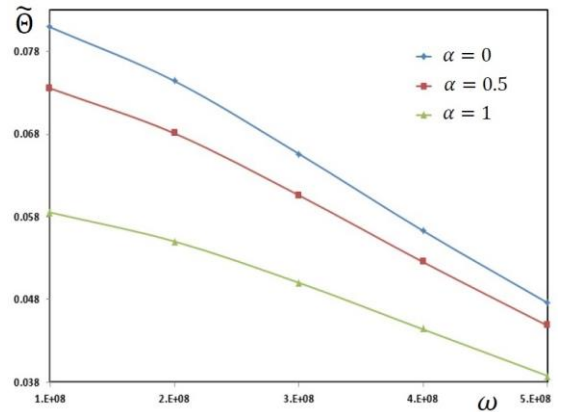


Fig. 9 The beam rotation $\tilde{\Theta}$ of sandwich microbeam in terms of excitation frequency ω for various first dimensionless material length scale parameters α .

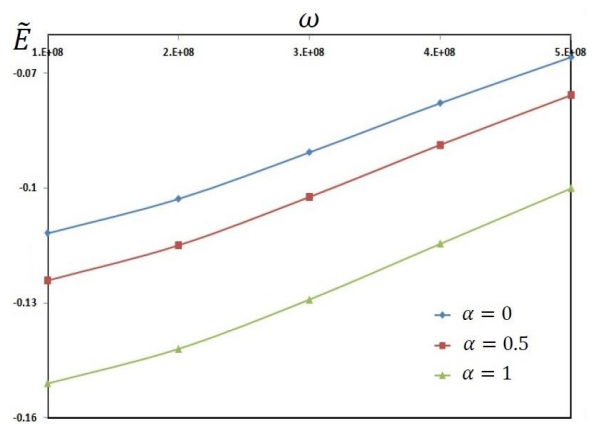


Fig. 10 The beam higher-order rotation \tilde{E} of sandwich microbeam in terms of excitation frequency ω for various first dimensionless material length scale parameters α .

It is observed that with increase of spring parameters of foundation, the non-dimensional displacement \bar{w} is decreased significantly. Fig. 5 shows the beam rotation $\tilde{\Theta} = 10^6\Theta$ of sandwich microbeam in terms of excitation frequency ω for various Winkler's parameters of foundation K_1 . One can conclude that with increase of Winkler's parameters of foundation K_1 , the stiffness of foundation is increased and consequently deflection and rotation of microbeam are decreased. Shown in Figure 6 is beam higher-order rotation $\tilde{E} = 10^6E$ of sandwich microbeam in terms of excitation frequency ω for various Winkler's parameters of foundation K_1 . One can see that beam higher-order rotation \tilde{E} of sandwich microbeam is negative and is decreased with increase of Winkler's parameters of foundation K_1 . Fig. 7 shows maximum electric potential $\tilde{\Psi} = 10^6\Psi$ through thickness direction of sandwich microbeam in terms of excitation frequency ω for various Winkler's parameters of foundation K_1 .

Fig. 8 shows non-dimensional displacement \bar{w} of sandwich microbeam in terms of excitation frequency ω for various first dimensionless material length scale parameter α . It can be concluded that with increase of first dimensionless material length scale parameter α , the dimensionless deflection is decreased due to increase of stiffness of structure. The influence of first dimensionless material length scale parameter α on the beam rotation $\tilde{\Theta}$, beam higher-order rotation \tilde{E} and maximum electric potential $\tilde{\Psi}$ through thickness direction of sandwich microbeam are presented in Figs. 9-11.

Influence of second dimensionless material length scale parameter β on the non-dimensional displacement \bar{w} of sandwich microbeam, beam rotation $\tilde{\Theta}$, beam higher-order rotation \tilde{E} and maximum electric potential $\tilde{\Psi}$ through thickness direction of sandwich microbeam in terms of excitation frequency ω are presented in Figs. 12-15.

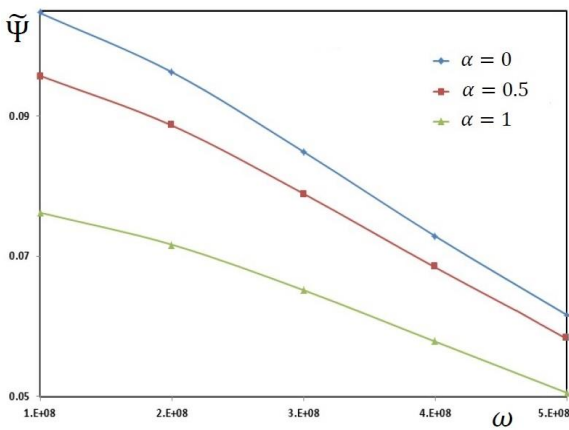


Fig. 11 The maximum electric potential $\tilde{\Psi}$ through thickness direction of sandwich microbeam in terms of excitation frequency ω for various first dimensionless material length scale parameters α

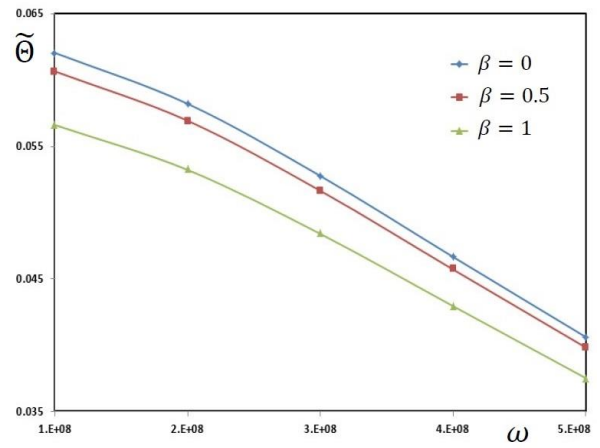


Fig. 13 The beam rotation $\tilde{\Theta}$ of sandwich microbeam in terms of excitation frequency ω for various second dimensionless material length scale parameters β

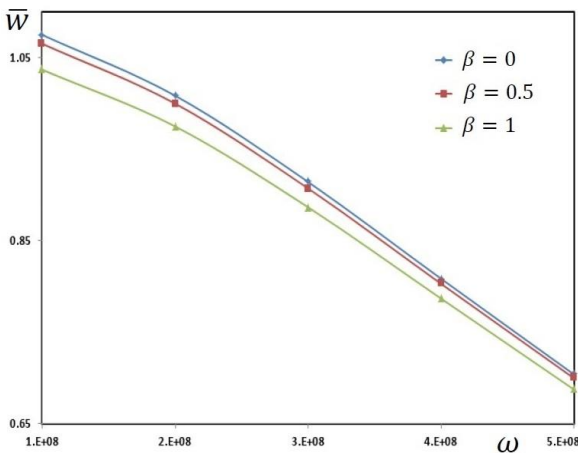


Fig. 12 The non-dimensional displacement \bar{w} of sandwich microbeam in terms of excitation frequency ω for various second dimensionless material length scale parameters β

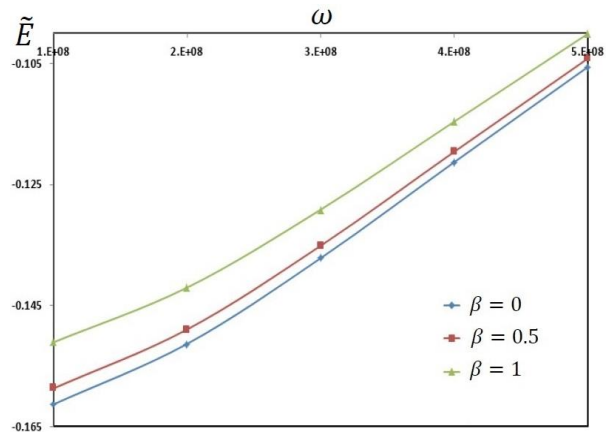


Fig. 14 The beam higher-order rotation \tilde{E} of sandwich microbeam in terms of excitation frequency ω for various second dimensionless material length scale parameters β

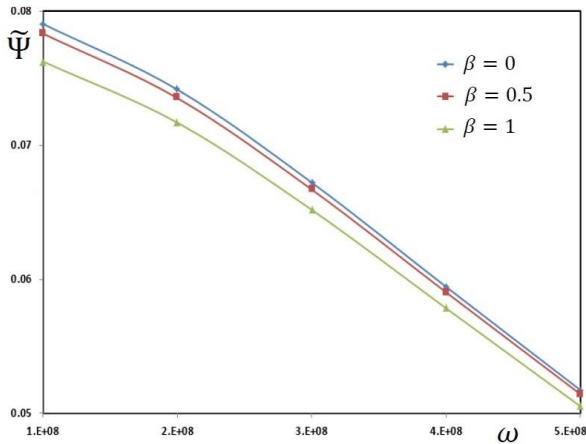


Fig. 15 The maximum electric potential $\tilde{\Psi}$ through thickness direction of sandwich microbeam in terms of excitation frequency ω for various second dimensionless material length scale parameters β

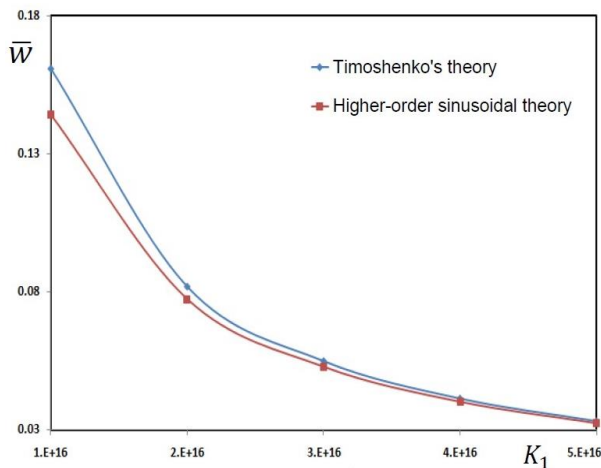


Fig. 16 Comparison of dimensionless deflection of microbeam between Timoshenko and higher-order sinusoidal shear deformation theories

Fig. 16 shows comparison of dimensionless deflections of microbeam between Timoshenko and higher-order sinusoidal shear deformation theories in terms of Winkler's parameters of foundation. It is concluded that employing the higher-order sinusoidal shear deformation theory can improve accuracy of results.

5. Conclusions

In this research, free vibration dynamic response analyses of a sandwich microbeam were investigated. The sandwich microbeam was fabricated from a micro-core and two integrated piezoelectric face sheets. Strain gradient theory as well as higher sinusoidal shear deformation beam theory were employed to derive governing equations of motion. After derivation of appropriate terms for kinetic and strain energies and energy due to external works, the

governing equations of motion were derived using Hamilton's principle. The important results to present the effect of significant parameters such as micro-length scale parameters, parameters of foundation and excitation frequency were presented. The main conclusions of this paper can be presented as follows:

Our analytical results indicate that material length scale parameters have significant effect on the vibration and dynamic characteristics of sandwich microbeam. To investigate the effect of three micro-length scale parameters (l_0, l_1, l_2) on the results, two dimensionless parameters $\alpha = l_1/l_0$ and $\beta = l_2/l_0$ were employed. The results show that fundamental frequencies are increased with increase of α while with increase of β , they increased for $\beta \leq 0.5$ and decreased for $\beta > 0.5$. In addition, with increase of two parameters of Pasternak's foundation, natural frequencies are increased significantly due to increase of stiffness.

Maximum electric potential through thickness direction of microbeam are changed with change of two dimensionless parameters α, β . It is concluded that with increase of α, β this component is decreased significantly. In addition, with increase of two parameters of foundation, maximum electric potential is decreased due to increase of stiffness of microbeam. The numerical results show that the beam higher-order rotation of microbeam is negative while the beam rotation is positive. Both components are decreased with increase of two parameters of Pasternak's foundation and two dimensionless material length scale parameters α, β .

Acknowledgments

The research described in this paper was financially supported by the University of Kashan. (Grant Number: 36346/5). They would also like to thank the Iranian Nanotechnology Development Committee for their financial support.

References

- Al-Basyouni, K.S., Tounsi, A. and Mahmoud, S.R. (2015), "Size dependent bending and vibration analysis of functionally graded micro beams based on modified couple stress theory and neutral surface position", *Compos. Struct.*, **125**, 621-630.
- Abdelaziz, H.H., Meziane, M.A.A., Bousahla, A.A., Tounsi, A., Mahmoud, S.R. and Alwabli, A.S. (2017), "An efficient hyperbolic shear deformation theory for bending, buckling and free vibration of FGM sandwich plates with various boundary conditions", *Steel Compos. Struct.*, **25**(6), 693-704.
- Abualnour, M., Houari, M.S.A., Tounsi, A., Bedia, E.A.A. and Mahmoud, S.R. (2018), "A novel quasi-3D trigonometric plate theory for free vibration analysis of advanced composite plates", *Compos. Struct.*, **184**, 688-697.
- Ahouel, M., Houari, M.S.A., AddaBedia, E.A. and Tounsi, A. (2016), "Size-dependent mechanical behavior of functionally graded trigonometric shear deformable nanobeams including neutral surface position concept", *Steel Compos. Struct.*, **20**(5), 963-981.
- Arefi, M., Rahimi, G.H. and Khoshgoftar, M.J. (2011),

- “Optimized design of a cylinder under mechanical, magnetic and thermal loads as a sensor or actuator using a functionally graded piezomagnetic material”, *Int. J. Phys. Sci.*, **6** (27), 6315-6322.
- Arefi, M. and Rahimi, G.H. (2011a), “Thermo elastic analysis of a functionally graded cylinder under internal pressure using first order shear deformation theory”, *Sci. Res. Essays.*, **5**(12), 1442-1454.
- Arefi, M. and Rahimi, G.H. (2011b), “Nonlinear analysis of a functionally graded square plate with two smart layers as sensor and actuator under normal pressure”, *Smart. Struct. Syst.*, **8** (5), 433-447.
- Arefi, M. and Rahimi, G.H., (2012a), “Comprehensive thermoelastic analysis of a functionally graded cylinder with different boundary conditions under internal pressure using first order shear deformation theory”, *Mechanika*, **18**(1), 5-13.
- Arefi, M. and Rahimi, G.H. (2012b) “The effect of nonhomogeneity and end supports on the thermo elastic behavior of a clamped–clamped FG cylinder under mechanical and thermal loads”, *Int. J. Pres. Ves. Pip.*, **96**, 30-37
- Arefi, M. and Rahimi, G.H. (2012c), “Studying the nonlinear behavior of the functionally graded annular plates with piezoelectric layers as a sensor and actuator under normal pressure”, *Smart. Struct. Syst.*, **9**(2), 127-143.
- Arefi, M., Rahimi, G.H. and Khoshgoftar, M.J., (2012), “Exact solution of a thick walled functionally graded piezoelectric cylinder under mechanical, thermal and electrical loads in the magnetic field”, *Smart. Struct. Syst.*, **9**(5), 427-439.
- Arefi, M. and Rahimi, G.H. (2014a) “Application of shear deformation theory for two dimensional electro-elastic analysis of a FGP cylinder”, *Smart. Struct. Syst.*, **13**(1), 1-24
- Arefi, M. and Rahimi, G.H. (2014b), “Comprehensive piezo-thermo-elastic analysis of a thick hollow spherical shell”, *Smart. Struct. Syst.*, **14**(2), 225-246.
- Arefi, M. (2014), “A complete set of equations for piezo-magnetoelastic analysis of a functionally graded thick shell of revolution”, *Latin. Am. J. Solids. Struct.*, **11**(11), 2073-2092.
- Arefi, M. and Allam, M.N.M. (2015), “Nonlinear responses of an arbitrary FGP circular plate resting on foundation”, *Smart. Struct. Syst.*, **16**(1), 81-100.
- Arefi, M. (2015), “Nonlinear electromechanical analysis of a functionally graded square plate integrated with smart layers resting on Winkler-Pasternak foundation”, *Smart. Struct. Syst.*, **16**(1), 195-211.
- Arefi, M. (2016a), “Surface effect and non-local elasticity in wave propagation of functionally graded piezoelectric nano-rod excited to applied voltage”, *Appl. Math. Mech. Engl. Ed.*, **37**, 289-302.
- Arefi, M. (2016b), “Analysis of wave in a functionally graded magneto-electro-elastic nano-rod using nonlocal elasticity model subjected to electric and magnetic potentials”, *Acta Mech.*, **227**, 2529-2542.
- Arefi, M. and Zenkour, A.M. (2016a), “A simplified shear and normal deformations nonlocal theory for bending of functionally graded piezomagnetic sandwich nanobeams in magneto-thermo-electric environment”, *J. Sandw. Struct. Mater.*, **18**, 624-651.
- Arefi, M. and Zenkour, A.M. (2016b), “Free vibration, wave propagation and tension analyses of a sandwich micro/nano rod subjected to electric potential using strain gradient theory”, *Mater. Res. Exp.*, **3**(11), 115704.
- Arefi, M., Karroubi, R. and Irani-Rahaghi, M. (2016a), “Free vibration analysis of functionally graded laminated sandwich cylindrical shells integrated with piezoelectric layer”, *Appl. Math. Mech.*, **3**(7), 821-834.
- Arefi, M., Abbasi, A.R. and Vaziri Sereshk, M.R. (2016b), “Two-dimensional thermoelastic analysis of FG cylindrical shell resting on the Pasternak foundation subjected to mechanical and thermal loads based on FSDT formulation”, *J. Therm. Stresses*, **39**(5), 554-570.
- Arefi, M., Faegh, R.K. and Loghman, A. (2016c), “The effect of axially variable thermal and mechanical loads on the 2D thermoelastic response of FG cylindrical shell”, *J. Therm. Stresses*, **39**(12), 1539-1559.
- Arefi, M. and Zenkour, A.M. (2017a), “Transient sinusoidal shear deformation formulation of a size-dependent three-layer piezomagnetic curved nanobeam”, *Acta. Mech.*, **228**(10), 3657-3674.
- Arefi, M. and Zenkour A.M. (2017b), “Thermo-electro-mechanical bending behavior of sandwich nanoplate integrated with piezoelectric face-sheets based on trigonometric plate theory”, *Compos. Struct.*, **162**, 108-122.
- Arefi, M. and Zenkour A.M. (2017c), “Nonlocal electro-thermo-mechanical analysis of a sandwich nanoplate containing a Kelvin–Voigt viscoelastic nanoplate and two piezoelectric layers”, *Acta Mech.*, **228**, 475-493.
- Arefi, M. and Zenkour A.M. (2017d), “Size-dependent vibration and bending analyses of the piezomagnetic three-layer nanobeams”, *Appl. Phys. A.*, **123**, 202.
- Arefi, M. and Zenkour A.M. (2017e), “Vibration and bending analysis of a sandwich microbeam with two integrated piezomagnetic face-sheets”, *Compos. Struct.*, **159**, 479-490.
- Arefi, M. and Zenkour, A.M. (2017f), “Influence of magneto-electric environments on size-dependent bending results of three-layer piezomagnetic curved nanobeam based on sinusoidal shear deformation theory”, *J. Sandw. Struct. Mater.*, In Press.
- Arefi, M. and Zenkour, A.M. (2017g), “Influence of micro-length-scale parameters and inhomogeneities on the bending, free vibration and wave propagation analyses of a FG Timoshenko’s sandwich piezoelectric microbeam”, *J. Sandwich Struct. Mater.* 1099636217714181
- Arefi, M. and Zenkour, A.M. (2017h), “Wave propagation analysis of a functionally graded magneto-electro-elastic nanobeam rest on Visco-Pasternak foundation”, *Mech. Res. Commun.*, **79**, 51-62.
- Arefi, M. and Zenkour, A.M. (2017i), “Effect of thermo-magneto-electro-mechanical fields on the bending behaviors of a three-layered nanoplate based on sinusoidal shear-deformation plate theory”, *J. Sandw. Struct. Mater.*, Doi: 1099636217697497.
- Arefi, M. and Zenkour, A.M. (2017j), “Employing the coupled stress components and surface elasticity for nonlocal solution of wave propagation of a functionally graded piezoelectric Love nanorod model”, *J. Intel. Mat. Syst. Str.*, **28**(17), 2403-2413.
- Arefi, M. Zamani, M.H. and Kiani, M., (2017), “Size-dependent free vibration analysis of three-layered exponentially graded nanoplate with piezomagnetic face-sheets resting on Pasternak’s foundation”, *J. Intel. Mat. Syst. Str.*, **29** (5), 774-786.
- Arefi, M. (2018a), “Buckling analysis of the functionally graded sandwich rectangular plates integrated with piezoelectric layers under bi-axial loads”, *J. Sandw. Struct. Mater.*, **19** (6), 712-735.
- Arefi, M. (2018b), “Analysis of a doubly curved piezoelectric nano shell: Nonlocal electro-elastic bending solution”, *Euro. J. Mech. A – Solids*, **70**, 226-237
- Attia, A., Tounsi, A., Adda Bedia, E.A. and Mahmoud, S.R. (2015), “Free vibration analysis of functionally graded plates with temperature-dependent properties using various four variable refined plate theories”, *Steel Compos. Struct.*, **18**(1), 187-212.
- Aydogdu, M. (2009), “Axial vibration of the nanorods with the nonlocal continuum rod model”, *Physica. E.*, **41**, 861-864.
- Bennoun, M., Houari, M.S.A. and Tounsi, A. (2016), “A novel five variable refined plate theory for vibration analysis of functionally graded sandwich plates”, *Mech. Adv. Mater. Struct.*, **23**(4), 423-431.
- Bessegghier, A., Houari, M.S.A., Tounsi, A. and Mahmoud, S.R.

- (2017), "Free vibration analysis of embedded nanosize FG plates using a new nonlocal trigonometric shear deformation theory", *Smart Struct. Syst.*, **19**(6), 601 - 614.
- Beldjelili, Y., Tounsi, A. and Mahmoud, S.R. (2016), "Hygro-thermo-mechanical bending of S-FGM plates resting on variable elastic foundations using a four-variable trigonometric plate theory", *Smart Struct. Syst.*, **18**(4), 755-786.
- Belkorissat, I., Houari, M.S.A., Tounsi, A., Adda Bedia, E.A., Mahmoud, S.R. (2015), "On vibration properties of functionally graded nano-plate using a new nonlocal refined four variable model", *Steel Compos. Struct.*, **18**(4), 1063-1081.
- Bellifa, H., Benrahou, K.H., Bousahla, A.A., Tounsi, A. and Mahmoud, S.R. (2017), "A nonlocal zeroth-order shear deformation theory for nonlinear postbuckling of nanobeams", *Struct. Eng. Mech.*, **62**(6), 695 -702.
- Bounouara, F., Benrahou, K.H., Belkorissat, I. and Tounsi, A. (2016), "A nonlocal zeroth-order shear deformation theory for free vibration of functionally graded nanoscale plates resting on elastic foundation", *Steel Compos. Struct.*, **20**(2), 227-249.
- Bouafia, K. Kaci, A. Houari, M.S.A. Benzair and A. Tounsi, A. (2017), "A nonlocal quasi-3D theory for bending and free flexural vibration behaviors of functionally graded nanobeams", *Smart Struct. Syst.*, **19**(2), 115-126.
- Bouderba, B., Houari, M.S.A., Tounsi, A. and Mahmoud, S.R. (2016), "Thermal stability of functionally graded sandwich plates using a simple shear deformation theory", *Struct. Eng. Mech.*, **58**(3), 397-422.
- Bourada, M., Kaci, A., Houari, M.S.A. and Tounsi, A. (2015), "A new simple shear and normal deformations theory for functionally graded beams", *Steel Compos. Struct.*, **18**(2), 409-423.
- Bousahla, A.A. Benyoucef, S. Tounsi, A. and Mahmoud, S.R. (2016), "On thermal stability of plates with functionally graded coefficient of thermal expansion", *Struct. Eng. Mech.*, **60**(2), 313-335.
- Chaht, F.L., Kaci, A., Houari, M.S.A., Tounsi, A., Beg, O.A. and Mahmoud, S.R. (2015), "Bending and buckling analyses of functionally graded material (FGM) size-dependent nanoscale beams including the thickness stretching effect", *Steel Compos. Struct.*, **18**(2), 425-442.
- El-Haina, F., Bakora, A., Bousahla, A.A., Tounsi, A. and Mahmoud, S.R. (2017), "A simple analytical approach for thermal buckling of thick functionally graded sandwich plates", *Struct. Eng. Mech.*, **63**(5), 585-595.
- Eringen, A.C. (1983), "On differential equations of nonlocal elasticity and solutions of screw dislocation and surface waves", *J. Appl. Phys.*, **54**, 4703-4710.
- Farokhi, H. and Ghayesh, M.H. (2015), "Nonlinear motion characteristics of microarches under axial loads based on modified couple stress theory", *Arch. Civil. Mech. Eng.*, **15**, 401-411.
- Farajpour, A., Hairi Yazdi, M.R. Rastgoo, A., Loghmani, M. Mohammadi, M. (2016), "Nonlocal nonlinear plate model for large amplitude vibration of magneto-electro-elastic nanoplates", *Compos. Struct.*, **140**, 323-336.
- Ghannadpour, S. A. M. Mohammadi, B. (2010), "Buckling analysis of micro- and nano-rods/tubes based on nonlocal Timoshenko beam theory using Chebyshev polynomials", *Adv. Mater. Res.* **123**, 619-622.
- Güven, U.A. (2014), "Generalized nonlocal elasticity solution for the propagation of longitudinal stress waves in bars", *Euro. J. Mech. A. Solids*, **45**, 75-79.
- Hamidi, A., Houari, M.S.A., Mahmoud, S.R. and Tounsi, A. (2015), "A sinusoidal plate theory with 5-unknowns and stretching effect for thermomechanical bending of functionally graded sandwich plates", *Steel Compos. Struct.*, **18**(1), 235-253.
- Houari, M.S.A., Tounsi, A., Bessaim, A. and Mahmoud, S.R. (2016), "A new simple three-unknown sinusoidal shear deformation theory for functionally graded plates", *Steel Compos. Struct.*, **22**, 257-276.
- Khetir, H., Bouiadjra, M.B., Houari, M.S.A., Tounsi, A. and Mahmoud, S.R. (2017), "A new nonlocal trigonometric shear deformation theory for thermal buckling analysis of embedded nanosize FG plates", *Struct. Eng. Mech.*, **64**(4), 391-402.
- Khoshgoftar, M.J. Rahimi, G.H. and Arefi, M. (2013), "Solution of functionally graded thick cylinder with finite length under longitudinally non-uniform pressure", *Mech. Res. Commun.*, **51**, 61-66.
- Larbi Chaht, F., Kaci, A., Houari, M.S.A., Tounsi, A., Anwar Bég, O. and Mahmoud, S.R. (2015), "Bending and buckling analyses of functionally graded material (FGM) size-dependent nanoscale beams including the thickness stretching effect", *Steel Compos. Struct.*, **18**(2), 425-442.
- Mahi, A., Bedia, E.A.A. and Tounsi, A. (2015), "A new hyperbolic shear deformation theory for bending and free vibration analysis of isotropic, functionally graded, sandwich and laminated composite plates", *Appl. Math. Model.*, **39**, 2489-2508.
- Meziane, M.A.A., Abdelaziz, H.H. and Tounsi, A. (2014), "An efficient and simple refined theory for buckling and free vibration of exponentially graded sandwich plates under various boundary conditions", *J. Sandw. Struct. Mater.*, **16**(3), 293-318.
- Menasria, A., Bouhadra, A., Tounsi, A., Bousahla, A.A. and Mahmoud, S.R. (2017), "A new and simple HSDT for thermal stability analysis of FG sandwich plates", *Steel Compos. Struct.*, **25**(2), 157-175.
- Mouffoki, A., Bedia, E.A.A., Houari, M.S.A., Tounsi, A. and Mahmoud, S.R. (2017), "Vibration analysis of nonlocal advanced nanobeams in hygro-thermal environment using a new two-unknown trigonometric shear deformation beam theory", *Smart Struct. Syst.*, **20**(3), 369-383.
- Park, S.K. and Gao, X.L. (2006), "Bernoulli-Euler beam model based on a modified couple stress theory", *J. Micromech. Microeng.*, **16**, 2355-2359.
- Pradhan, K.K. and Chakraverty, S. (2013), "Free vibration of Euler and Timoshenko functionally graded beams by Rayleigh-Ritz method", *Compos. Part. B.*, **51**, 175-184.
- Rahimi, G.H., Arefi, M. and Khoshgoftar, M.J., (2012), "Electro elastic analysis of a pressurized thick-walled functionally graded piezoelectric cylinder using the first order shear deformation theory and energy method", *Mechanika*, **18**(3), 292-300.
- Sahmani, S. and Ansari, R. (2013), "On the free vibration response of functionally graded higher-order shear deformable microplates based on the strain gradient elasticity theory", *Compos. Struct.*, **95**, 430-442.
- Shooshtari, A. and Rafiee, M. (2011), "Nonlinear forced vibration analysis of clamped functionally graded beams", *Acta. Mech.*, **221**, 23-38.
- Song, J. Shen, J. and Li, X.F. (2010), "Effects of initial axial stress on waves propagating in carbon nanotubes using a generalized nonlocal model", *Comput. Mater. Sci.*, **49**, 518-523.
- Sourki, R. and Hoseini, S.A.H. (2016), "Free vibration analysis of size-dependent cracked microbeam based on the modified couple stress theory", *Appl. Phys. A.*, **122**, 413.
- Tounsi, A., Houari, M.S.A., Benyoucef, S. and Adda Bedia, E.A. (2013), "A refined trigonometric shear deformation theory for thermoelastic bending of functionally graded sandwich plates", *Aerosp. Sci. Technol.*, **24**, 209-220.
- Wang, B., Zhao, J. and Zhou, S. (2010), "A micro scale Timoshenko beam model based on strain gradient elasticity theory", *Euro. J. Mech. A. Solids*, **29**, 591-599.
- Wang, C.M. (1995), "Timoshenko beam bending solutions in terms of Euler-Bernoulli solutions", *J. Eng. Mech.*, **121**, 763-

765.

- Zenkour, A.M. and Arefi, M. (2017), "Nonlocal transient electrothermomechanical vibration and bending analysis of a functionally graded piezoelectric single-layered nanosheet rest on visco-Pasternak foundation", *J. Therm. Stresses*, **40**, 167-184.
- Zemri, A., Houari, M.S.A., Bousahla, A.A. and Tounsi, A. (2015), "A mechanical response of functionally graded nanoscale beam: an assessment of a refined nonlocal shear deformation theory beam theory", *Struct. Eng. Mech.*, **54**(4), 693-710.
- Zhang, L. Wang, B. Zhou, S. and Xue, Y. (2017), "Modeling the Size-Dependent Nanostructures: Incorporating the Bulk and Surface Effects", *J. Nanomech. Micromech.*, **7**, 37-47.
- Zhen, Y. (2016), "Vibration and Instability Analysis of Double-Carbon Nanotubes System Conveying Fluid", *J. Nanomech. Micromech.*, **6**, 25-41.

CC

Appendix

$$\{J_7, J_8, J_{10}, J_{23}, J_{27}, J_{37}\} = \int_{\frac{h}{2}-h_p}^{\frac{h}{2}} C_{1111}\{1, x_3, x_3^2, \chi, \chi x_3, \chi^2\} dx_3 \\ + \int_{\frac{h}{2}}^{\frac{h}{2}+h_p} E\{1, x_3, x_3^2, \chi, \chi x_3, \chi^2\} dx_3 + \\ \int_{\frac{h}{2}}^{\frac{h}{2}+h_p} C_{1111}\{1, x_3, x_3^2, \chi, \chi x_3, \chi^2\} dx_3,$$

$$\int_{\frac{h}{2}-h_p}^{\frac{h}{2}} \{1, x_3, \chi\} \frac{\pi}{h_p} e_{113} \sin\left(\frac{\pi \check{x}_3}{h_p}\right) dx_3 + \\ \int_{\frac{h}{2}}^{\frac{h}{2}+h_p} \{1, x_3, \chi\} \frac{\pi}{h_p} e_{113} \sin\left(\frac{\pi \hat{x}_3}{h_p}\right) dx_3,$$

$$\int_{\frac{h}{2}-h_p}^{\frac{h}{2}} C_{1313}\{1, \chi', \chi'^2\} dx_3 + \int_{\frac{h}{2}}^{\frac{h}{2}+h_p} G\{1, \chi', \chi'^2\} dx_3 + \\ \int_{\frac{h}{2}}^{\frac{h}{2}+h_p} C_{1313}\{1, \chi', \chi'^2\} dx_3,$$

$$\{J_{13}, J_{25}\} = \\ \int_{\frac{h}{2}-h_p}^{\frac{h}{2}} e_{131}\{1, \chi'\} \cos\left(\frac{\pi \check{x}_3}{h_p}\right) dx_3 + \int_{\frac{h}{2}}^{\frac{h}{2}+h_p} e_{131}\{1, \chi'\} \cos\left(\frac{\pi \hat{x}_3}{h_p}\right) dx_3,$$

$$J_{14} = \int_{\frac{h}{2}-h_p}^{\frac{h}{2}} \eta_{11} \left[\cos\left(\frac{\pi \check{x}_3}{h_p}\right) \right]^2 dx_3 + \int_{\frac{h}{2}}^{\frac{h}{2}+h_p} \eta_{11} \left[\cos\left(\frac{\pi \hat{x}_3}{h_p}\right) \right]^2 dx_3,$$

$$J_{15} = \int_{\frac{h}{2}-h_p}^{\frac{h}{2}} \eta_{33} \left[\frac{\pi}{h_p} \sin\left(\frac{\pi \check{x}_3}{h_p}\right) \right]^2 dx_3 \\ + \int_{\frac{h}{2}}^{\frac{h}{2}+h_p} \eta_{33} \left[\frac{\pi}{h_p} \sin\left(\frac{\pi \hat{x}_3}{h_p}\right) \right]^2 dx_3,$$

$$\{J_{16}, J_{17}, J_{18}, J_{28}, J_{29}, J_{30}, J_{35}, J_{36}\} \\ = \int_{\frac{h}{2}-h_p}^{\frac{h}{2}} 2\mu^p l_0^2 \{1, x_3, x_3^2, \chi, \chi', \chi x_3, \chi^2, \chi'^2\} dx_3 \\ + \int_{\frac{h}{2}}^{\frac{h}{2}+h_p} 2\mu l_0^2 \{1, x_3, x_3^2, \chi, \chi', \chi x_3, \chi^2, \chi'^2\} dx_3 + \\ \int_{\frac{h}{2}}^{\frac{h}{2}+h_p} 2\mu^p l_0^2 \{1, x_3, x_3^2, \chi, \chi', \chi x_3, \chi^2, \chi'^2\} dx_3,$$

$$\{J_{19}, J_{20}, J_{21}, J_{31}, J_{32}, J_{39}, J_{40}, J_{41}, J_{42}, J_{43}\} = \\ = \int_{\frac{h}{2}-h_p}^{\frac{h}{2}} 2\mu^p l_1^2 \{1, x_3, x_3^2, \chi, \chi x_3, \chi^2, \chi'', \chi'' x_3, \chi'' \chi, \chi''^2\} dx_3 \\ + \int_{\frac{h}{2}}^{\frac{h}{2}+h_p} 2\mu l_1^2 \{1, x_3, x_3^2, \chi, \chi x_3, \chi^2, \chi'', \chi'' x_3, \chi'' \chi, \chi''^2\} dx_3 \\ + \int_{\frac{h}{2}}^{\frac{h}{2}+h_p} 2\mu^p l_1^2 \{1, x_3, x_3^2, \chi, \chi x_3, \chi^2, \chi'', \chi'' x_3, \chi'' \chi, \chi''^2\} dx_3,$$

$$\{J_{22}, J_{33}, J_{34}\} = \int_{\frac{h}{2}-h_p}^{\frac{h}{2}} 2\mu^p l_2^2 \{1, \chi', \chi'^2\} dx_3 \\ + \int_{\frac{h}{2}}^{\frac{h}{2}+h_p} 2\mu l_2^2 \{1, \chi', \chi'^2\} dx_3 \\ + \int_{\frac{h}{2}}^{\frac{h}{2}+h_p} 2\mu^p l_2^2 \{1, \chi', \chi'^2\} dx_3,$$

$$D\psi = \\ \int_{\frac{h}{2}-h_p}^{\frac{h}{2}} 2\eta_{33} \frac{\pi}{h_p} \sin\left(\frac{\pi \check{x}_3}{h_p}\right) \frac{V_0}{h_p} dx_3 + \int_{\frac{h}{2}}^{\frac{h}{2}+h_p} 2\eta_{33} \frac{\pi}{h_p} \sin\left(\frac{\pi \hat{x}_3}{h_p}\right) \frac{V_0}{h_p} dx_3, \\ \{N\psi, M\psi, S\psi\} = \int_{\frac{h}{2}-h_p}^{\frac{h}{2}} 2e_{113} \frac{V_0}{h_p} \{1, x_3, \chi\} dx_3 + \\ \int_{\frac{h}{2}}^{\frac{h}{2}+h_p} 2e_{113} \frac{V_0}{h_p} \{1, x_3, \chi\} dx_3$$